Research Article

Estimation of particulate matter ($PM_{2.5}$, PM_{10}) concentration and its variation over urban sites in Bangladesh

Amitesh Gupta[1,2] · Md Moniruzzaman[3,4] · Avinash Hande[5] · Iman Rousta[6,7] · Haraldur Olafsson[8] · Karno Kumar Mondal[9]

Received: 27 July 2020 / Accepted: 3 November 2020 / Published online: 12 November 2020

Abstract
Satellite-retrieved aerosol optical depth essentially provides an economical option for regular monitoring of particulate matter (PM) concentration; however, the constrains and challenges come in terms of estimation accuracy. In the present study, we estimated $PM_{2.5}$ and PM_{10} (PM of aerodynamic diameter lesser than 2.5, 10 µm, respectively) for 11 sites in Bangladesh using different methods. Univariate model showed destitute performance ($R^2 < 0.1$), whereas integrating MODIS-AOD with surface meteorology, multivariate models enhanced accuracy ($R^2 > 0.6$); meanwhile, radial kernel-based 'eps'-type support vector regression model outperformed rest ($R^2 > 0.8$). Furthermore, we investigated variations in ground concentration of $PM_{2.5}$, PM_{10} during 2013–2018 and found annual mean concentration of 76.34 ± 34.12 µg m^{-3} and 136.25 ± 68.94 µg m^{-3}, respectively. Predominant anthropogenic contribution to elevated pollution is well remarked by $PM_{2.5}/PM_{10}$ ratio, highest during January (0.65 ± 0.06) and lowest during July (0.48 ± 0.11). Grievous pollution found in Narayanganj ($PM_{2.5}$: 100.35 ± 56.76 µg m^{-3}, PM_{10}: 200.25 ± 91.79 µg m^{-3}) and slightest in Sylhet ($PM_{2.5}$: 56.13 ± 26.99 µg m^{-3}, PM_{10}: 103.94 ± 49.37 µg m^{-3}). Intra-annual pattern asserts winter as sternly befouled and least pollution during monsoon, which may indicate significant influence of meteorology on PM pollution. We found that PM divulged negative correlation with air temperature ($PM_{2.5}$: −0.78, PM_{10}: −0.73), relative humidity ($PM_{2.5}$: −0.66, PM_{10}: −0.73) and rainfall ($PM_{2.5}$: −0.59, PM_{10}: −0.61). This study showed outrageous situation of PM pollution in urban areas in Bangladesh and proposed modest pathway for regular monitoring of PM that will help to combat pollution.

Keywords Particulate matter estimation · $PM_{2.5}$ · PM_{10} · Support vector regression · Radial kernel · MODIS AOD

1 Introduction

Over the last two decades, South Asian countries have attained a rapid economic growth, and in accordance with such developmental activities, excessive emergence of air pollutants has created a serious hazardous condition [1, 2]. Among major pollutants, particulate matter (PM) has been held responsible for several health problems mostly for respiratory and cardiovascular diseases [3–7]. PM with diameter of less than 10 µm is known as respirable suspended particulate matter (RSPM), while $PM_{2.5}$ has diameter of less than 2.5 µm, also known as suspended particulate matter (SPM). Depending on the meteorological conditions, $PM_{2.5}$ and PM_{10} can change their physical and chemical properties and able to remain suspended in the air for moderate to longer duration, thus having the

✉ Amitesh Gupta, amitesh13gupta14@gmail.com | [1]JIS University, Kolkata, India. [2]Indian Institute of Remote Sensing, Dehradun, India. [3]ASICT Division, Bangladesh Agricultural Research Institute, Gazipur, Bangladesh. [4]Center for Space Science and Technology Education in Asia and the Pacific, Dehradun, India. [5]Savitribai Phule Pune University, Pune, India. [6]Yazd University, Yazd, Iran. [7]Institute for Atmospheric Sciences -Weather and Climate, Meteorological Office, University of Iceland and Icelandic, Reykjavik, Iceland. [8]Department of Physics, Institute for Atmospheric Sciences Weather and Climate, Meteorological Office, University of Iceland and Icelandic, Reykjavik, Iceland. [9]Khulna University of Engineering and Technology, Khulna, Bangladesh.

potentiality to alter the radiative balance of the atmosphere directly and indirectly from a local to regional scale, which might have an adverse effect on the climate and environment [8–11]. Along with meteorological conditions, long-range transportation over the landmass during the winter season and small-range local scale dispersion from local sources of pollution also contribute to make surrounding air unhealthier [12–15]. Several studies such as [16–20] have reported that these PM are usually generated from daily activity-based common sources such as the transportation sector (vehicular emission), industrial sector (emissions from chimneys), household uses (usage of coals, woods or oil as fuel). Thus, exponential increase of anthropogenic activities due to rapid urbanization often held responsible for the deterioration of air quality during the last 2 decades [21–25], mostly over the urban areas with higher population density [26–28]. The capital of Bangladesh, Dhaka, witnessed such worsening of air quality since PM concentration was found to be higher than the Bangladesh National Ambient Air Quality Standard (BNAAQS) on a regular basis for more than 75% of the days in a year, thus, ranked among the topmost air polluted cities in the world [29, 30]. However, there are significant variations in measured PM levels over different locations in Bangladesh [31]. During the rainy season, the pollution level was noticed to be below the annual mean over most of the locations, while during rest of the months, the sites of Dhaka, Gazipur, and Narayanganj register multi-fold higher values than BNAAQS limit [32]. A detailed study by [33] found recursively high annual mean concentrations of PM_{10} (> 150 μg m^{-3}) over Dhaka, Gazipur and Narayanganj during 2012–2015. Annual mean concentration of 80–100 μg m^{-3} for $PM_{2.5}$ and 140–200 μg m^{-3} for PM_{10} was recorded during 2013–2017 over Darus Salam, Narayanganj and Gazipur [34]. Therefore, all of these major studies propound an importance of regular monitoring of PM over larger regional extent which can only be possible using satellite data, because with the ground network only point level or local scale information can be acquired which does not need to be the same over regional extent [35]. Besides, the variations in ground observed PM levels also need to be investigated in a nation-wide scale.

During the last 2 decades, satellite-retrieved aerosol optical depth (AOD) has been extensively used as a tool for measuring air pollution [36–43]. Satellite-based AOD has been regularly retrieved from different sensors from polar orbiting platform such as moderate-resolution imaging spectroradiometer (MODIS), visible infrared imaging radiometer suite (VIIRS), cloud-aerosol lidar with orthogonal polarization (CALIOP), multi-angle imaging spectroradiometer (MISR), ozone monitoring instrument (OMI) and polarization and directionality of the earth's reflectance (POLDER) [44–48]. AOD is retrieved from each sensors using different algorithms for processing. MODIS employs 3 different aerosol retrieval algorithms for AOD: dark target over land [49] for dark surfaces (vegetation), dark target over ocean [50] and deep blue which was initially developed for bright surfaces [51], later redeveloped for global land surface also [52]. A new generic aerosol algorithm, the multiangle implementation of atmospheric correction (MAIAC), which uses MODIS L1B time series measurements since 2000 and image processing to retrieve AOD at 1 km spatial resolution over land [53–55], 2018) has been operational with MODIS collection 6 products which is available as MCD19A2 (https://modis-land.gsfc.nasa.gov/MAIAC.html). The present study used this latest AOD product as well as it has been validated using ground observations over AErosol RObotic NETwork (AERONET) site in Dhaka for the study period of 2013–2018. Meanwhile, few investigations have used different local meteorological parameters to better correlate PM and AOD [56–62]. Hence, various methods have been implied in order to estimate PM, such as linear regression model [63–65], multiple linear regression model [66–70], generalised additive models [71–73], mixed effect model [74–76], geographically weighted regression [35, 76–78], while machine learning algorithm such as support vector regression (SVR) is least explored. However, SVR is found to be useful to resolve various geophysical complexity as this technique overcomes the limitations of linear dependency of input variables to estimate the output variable [79–81]. Therefore, in order to perform regular spatial monitoring, there is a need of a suitable technique to establish so that PM estimation can be done with better reliability. Till date, the PM pollution studies in Bangladesh had rarely focused on PM estimation using satellite dataset and surface meteorology. The present study aims to analyse and explore different methods with special preference to SVR model to estimate PM using $MODIS_{AOD}$ and local meteorology as well as looked in to the variations in ground measured PM and its dependency on local meteorology.

2 Data and methodology

2.1 CAMS site locations and ground data

The Department of Environment in Bangladesh has set up 11 continuous air quality monitoring stations (CAMS) in 8 different cities (Dhaka, Gazipur, Narayanganj, Sylhet, Chittagong, Barisal, Rajshahi and Khulna) in Bangladesh (Fig. 1). These monitoring network has been established over the major cities in Bangladesh where the population is more than 1 million and population density is more than 7500 person km^{-2}, i.e. more than 6 times higher of the national average (1253 person km^{-2}) [82]. The detailed

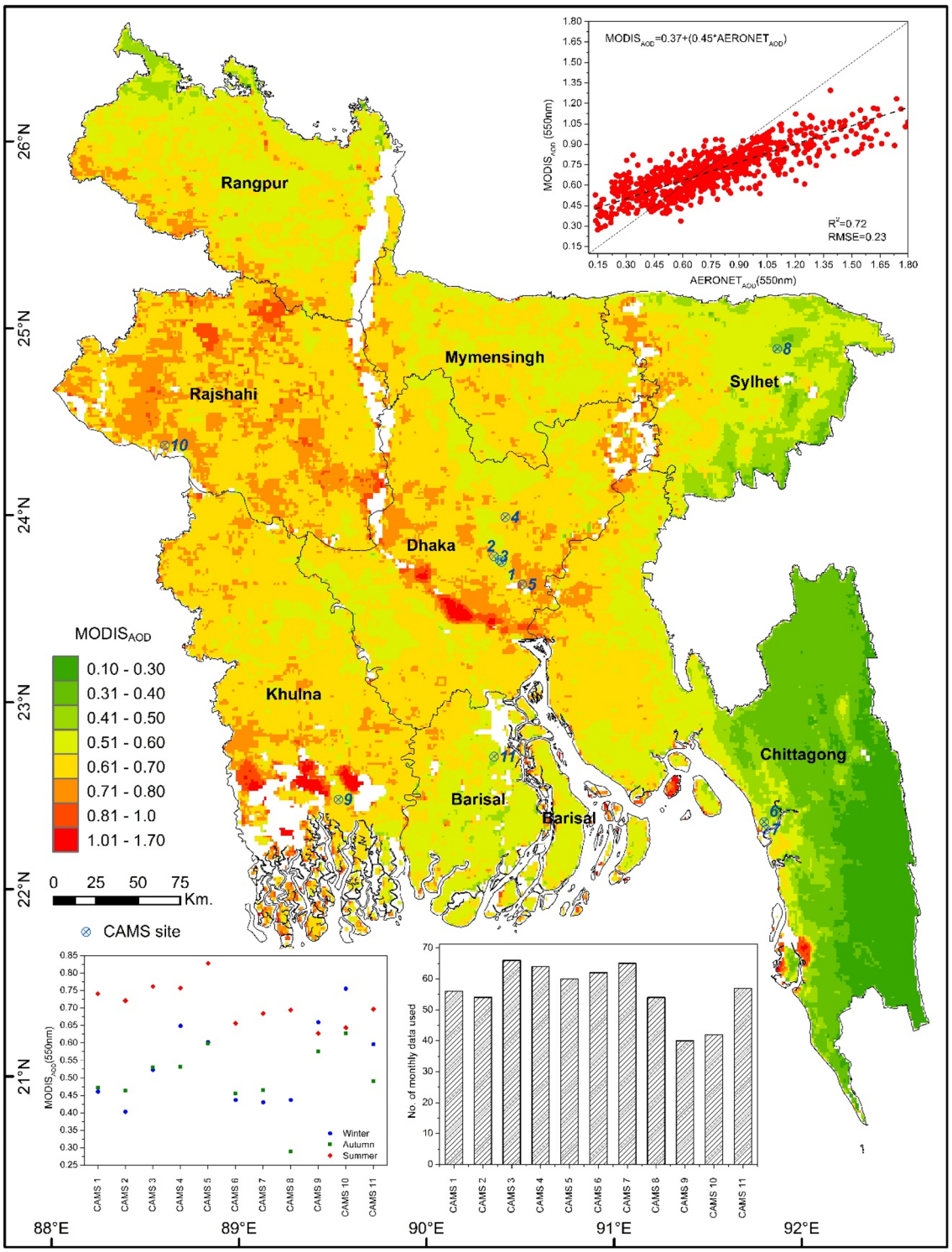

Fig. 1 Location of CAMS sites in Bangladesh. In background spatial distribution of annual mean MODIS-AOD during 2013–2018 over Bangladesh is shown. Number of monthly data used from each station, the validation (scatter graph) of MODIS-AOD with AERONETAOD over Dhaka and the seasonal pattern of MODIS-AOD over CAMS sites are shown in small graphs inside

site descriptions are available in technical report by [83]. CAMS measures surface concentration of major air pollutants such as $PM_{2.5}$, PM_{10}, CO, SO_2, NO_x and O_3 as well as keep records of meteorological parameters (e.g. solar radiation, temperature, humidity and rainfall). However, among these 11 locations, only 5 monitoring stations have

more than 80% of regular observation during January 2013 to December 2018, while the rest of the stations have 50–80% of observations during the same period. Hence, ground data from each station were screened on the basis of continuity of measurements and only those monthly data were taken when the continuity was at least 70%. The present study only incorporates meteorological data of air temperature (AT), relative humidity (RH) and rainfall (RF) with surface measurements of $PM_{2.5}$ and PM_{10}.

2.2 Prevailing meteorology over CAMS sites

Since all the monitoring stations are typically urban sites, the role of local meteorology must be considered [84–86]. Bangladesh is located in tropical monsoon region; hence, climatic pattern over CAMS sites also characterized by seasonal variation of meteorology during 4 distinct seasons (1) winter (December–February), (2) summer or premonsoon (March–May), (3) rainy season or monsoon (June–September) and (4) autumn or postmonsoon season (October–November) [87, 88]. The meteorological observations recorded over these monitoring stations are averaged and shown in Fig. 2a and b. It depicts hot and humid weather during summer, while cold and dry conditions during winter over those selected sites. Monthly mean of AT, RH and RF varies within a range of 18.25–30.51 °C, 55.55–87.29%, 0.04–12.67 cm, respectively, with an average of 26.65 °C, 72.51%, 3.77 cm during the study period. The maximum AT recorded in the month of June 2013, while the highest RH and RF were recorded in August 2015. Over these sites, the summer weather is distinguished by comparatively higher AT (28.09 °C) and RH (68.30%) but lesser RF (3.03 cm), while during the rainy season, AT drops very little (27.97 °C), but RF and RH increase significantly (8.05 cm, 80.99%, respectively). Autumn is characterized by 26.26 °C of AT, 1.31 cm RF and 72.70% RH, while the winter experience lesser AT, RF and RH (20.85 °C, 0.64 cm and 65.84%, respectively).

2.3 Satellite AOD

The MAIAC processing algorithm incorporates MODIS top-of-atmosphere L1B reflectance on a fixed grid of 1 km resolution as well as uses different band combinations, including 0.47, 0.55, 0.65 and 2.13 µm, depending on the surface brightness and the detected aerosol type [89], while the column water vapour (CWV) from MODIS NIR measurements at 0.94 µm [90] is used for atmospheric correction.

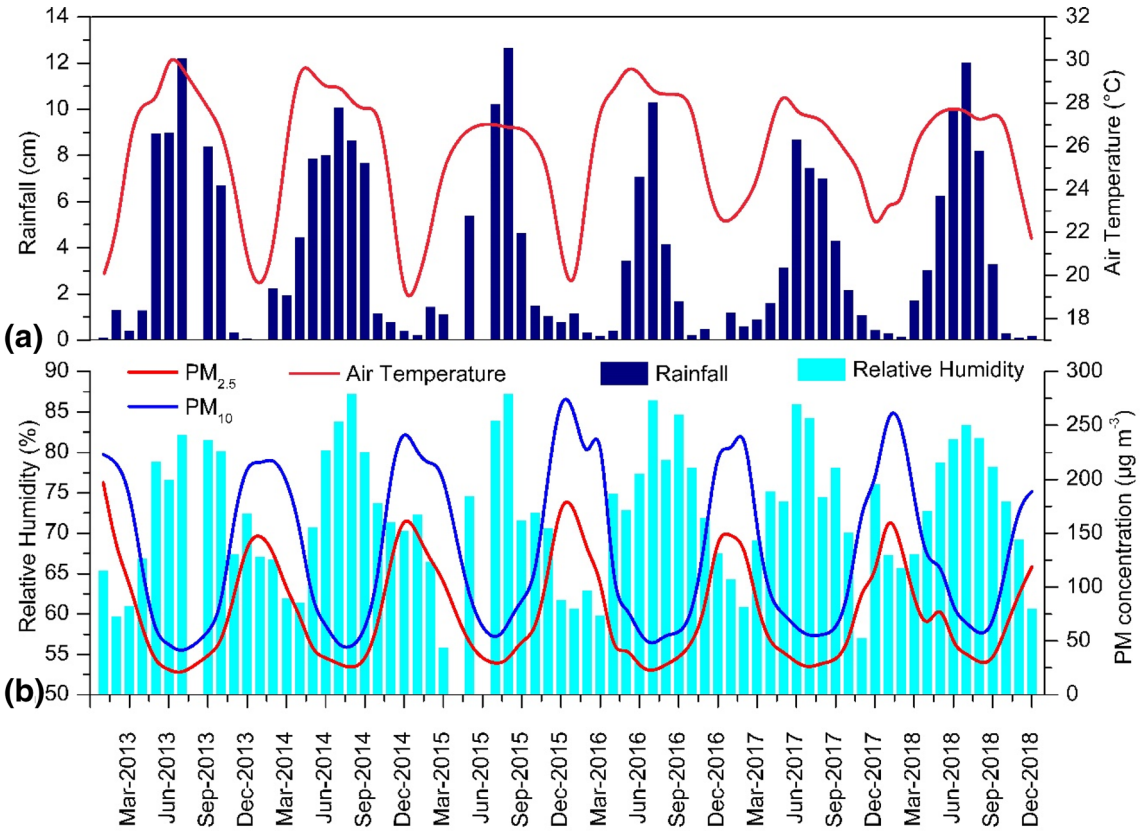

Fig. 2 **(a)** Prevailing meteorological conditions and (**b**) PM concentration over CAMS sites in Bangladesh

The MAIAC uses location-based aerosol models depending on the aerosol climatology obtained from AERONET. The current MAIAC aerosol models are static; hence, these do not consider seasonal variations of the aerosol properties, which is one of the limitations of the MAIAC C6 aerosol product. In this study, MODIS level-2 gridded (L2G) AOD data of 1 km. resolution was accessed from the Land Processes Distributed Active Archive Center (LP DAAC) for the study period.

2.4 Validation of satellite AOD

AERONET is a global ground-based sun photometer network which provides cloud screened AOD at several wavelengths between 340 and 1640 nm with high temporal resolution (5–15 min) [91]. Henceforth, AERONET version 2 level 2.0 quality-controlled AOD data at 500 nm were interpolated to 550 nm using angstrom exponent at 440 nm and 870 nm wavelength pair with the help of Eq. 1 and Eq. 2. Since MODIS provides spatial data of AOD once in a day, i.e. during the satellite overpass time only, thus, in order to compare the $\text{AERONET}_{\text{AOD}}$ with the $\text{MODIS}_{\text{AOD}}$, averaging has been done for $\text{AERONET}_{\text{AOD}}$ over a temporal window of ±60 min around the satellite overpass time and for $\text{MODIS}_{\text{AOD}}$ over a spatial window of 3 × 3 pixels centred at the AERONET site in Dhaka. Only the highest quality AOD data have been used to avoid cloud contamination and other errors that might held during the AOD retrieval. Here, we used the expected error (EE) of $\pm(0.05 + 0.20\ \text{AERONET}_{\text{AOD}})$.

$$\tau_{\lambda 1} = \tau_{\lambda 2} \times \left(\frac{\lambda 1}{\lambda 2}\right)^{-\alpha} \tag{1}$$

$$\alpha = -\frac{\ln\left(\frac{\tau_{\lambda 1}}{\tau_{\lambda 2}}\right)}{\ln\left(\frac{\lambda 1}{\lambda 2}\right)} \tag{2}$$

where $\tau_{\lambda 1}$, $\tau_{\lambda 2}$ are the AOD at the wavelength $\lambda 1$, $\lambda 2$, respectively, α is angstrom exponent.

2.5 Model approach for PM estimation

In order to investigate the interrelationship between AOD and PM, as well as the importance of meteorology to estimate the PM, several models had been critically explored. The selected dataset of 620 monthly observations from altogether 11 stations was subdivided into 3 parts—(a) training dataset, which accounts 70% of the total dataset used to construct each of the models, (b) 15% of the dataset included in testing dataset which is used to verify whether the constructed model is performing and (c) the rest 15% of dataset used for generation scatter plot for the validation purpose. Broadly, the experimented models can be categorized into 3 groups.

(1) Univariate model—here, interdependency of satellite AOD and PM had been checked using simple linear regression model (*M*1) (Eq. 3).

$$\text{PM} = i + \beta_{\text{AOD}}\text{AOD} \tag{3}$$

(2) Multivariate model—besides AOD, many studies carried over different places across the world have used several meteorological parameters with satellite AOD to estimate PM and found improved accuracy [92–94]. In the present study, we used $\text{MODIS}_{\text{AOD}}$, AT, RH and RF to estimate PM in *M*2 (Eq. 4). This approach helped to know whether the multiple linear regression is useful to estimate PM in the context of Bangladesh

$$\text{PM} = i + \beta_{AOD} \times \text{AOD} + \beta_{AT} \times AT + \beta_{RH} \times RH + \beta_{RF} \times RF \tag{4}$$

where i is intercept of the model, β_{AOD}, β_{AT}, β_{RH}, β_{RF} are the coefficient of AOD, AT, RH, RF, respectively.

(3) SVR model—the SVR, first introduced by [95], is one of the 2 main categories of support vector machine, after developed by [96], which implements a learning algorithm to the input data to recognize and generalize subtle patterns in any complex data set with the help of different kernels, thereafter predicting the depended variable of previously unseen data [97]. The fundamental concept of SVR is based on the computation of a regression function in a high-dimensional feature space where the input data are mapped via a nonlinear function. Overview of different algorithms used in SVR has been discussed in [98]. In the present study, we have used '*R*' platform, where 2 different types of SVR—'nu' and 'eps' were performed with 3 different kernels—linear, radial and polynomial, as well as in each case tenfold cross-validation was performed and accordingly the cost and gamma values were set. Basically, linear kernel (Eq. 5) is useful when dealing with large sparse data vectors, hence, most used in regression, while polynomial kernel (Eq. 6) is mostly used in such cases where the variance is not too high among neighbouring pixels and the input is normalized within a certain range value [99]. On the other hand, radial kernels (Eq. 7) transform a nonlinear dataset into several linear combinations in such a way that regression can be performed in several hyperplane over linearly transformed data. Thus, the kernels are simply different in case of making the hyperplane decision boundary among different input parameters [100], since these kernel functions map the original dataset into a higher-dimensional space

with a view to make it linear [101]. Usually linear and polynomial kernels are less time-consuming to perform but provide less accuracy than radial kernel [102, 103]. However, no such study has been carried to point out particularly which kernel is best for PM estimation. Therefore, incorporating these 3 kernels, SVR models (*M*3–*M*8) were analysed for estimating the PM. *M*3–*M*5 used 3 different kernels with 'eps' type of regression, while *M*6–*M*8 used the same 3 kernels with 'nu' type of regression.

$$K(x, y) = x^T y \tag{5}$$

$$K(x, y) = \left(1 + \sum_{j=1}^{p} x_{ij} y_{ij}\right)^d \sqrt{2} \tag{6}$$

$$K(x, y) = \exp\left(-\gamma \sum_{j=1}^{p} \left(x_{ij} - y_{ij}\right)^2\right) \tag{7}$$

where K is the corresponding kernel function, d is the degree of polynomial, and γ is the gamma function.

2.6 Statistical measures

Table 1 shows the descriptive statistics (mean, median, mode, standard deviation, standard error, range, minimum and maximum) of input variables used for regression analysis. Since values of $PM_{2.5}$ significantly differ from PM_{10}, thus to compare the accuracy by the same model for 2 different predicted variables having different value ranges, normalized statistical parameters would be meaningful to evaluate. Therefore, for assessing the estimation accuracy, coefficient of determination (R^2), normalized root-mean-square error (NRMSE) and normalized mean bias (NMB) have been used, and all of them vary between 0 and 1. R^2 signifies the explained variance of the model, NRMSE shows how much the data are scattered, thus indicating the absolute value of error while predicting the dependent variable, and NMB is used to estimate the average bias produced by the model and to decide the margin of prediction towards higher or lower than observation, i.e. the magnitude of overestimation or underestimation.

3 Results and discussion

3.1 PM concentration over CAMS sites

The average PM concentrations over selected sites during study period are shown in Fig. 2b. It depicts that the PM values tend to increase in those particular months when RH is comparatively lesser. Annual average $PM_{2.5}$ and PM_{10} concentrations over the sites were 76.34 ± 34.12 μg m^{-3} and 136.25 ± 68.94 μg m^{-3}, respectively. Meanwhile, $PM_{2.5}$ found highest (197.19 μg m^{-3}) during January 2013 and PM_{10} was highest (296.52 μg m^{-3}) during January 2019. CAMS-5 site in Narayanganj recorded highest annual mean concentration of $PM_{2.5}$ and PM_{10} (100.35 ± 56.76 μg m^{-3} and 200.25 ± 91.79 μg m^{-3}), while lowest annual mean $PM_{2.5}$ and PM_{10} concentration was recorded over CAMS-8 site in Sylhet (56.13 ± 26.99 μg m^{-3} and 103.94 ± 49.37 μg m^{-3}). It reveals that all monitoring stations are located in severely polluted areas, since the lowest concentrations were also much higher than the annual limit prescribed by BNAAQs (15 μg m^{-3} for $PM_{2.5}$ and 50 μg m^{-3} for PM_{10}). PM ratio (PMr), i.e. ratio of $PM_{2.5}$ and PM_{10}, signifies the amount of $PM_{2.5}$ contributing within PM_{10} concentration. It stipulates the substantial anthropogenic contribution to the PM concentration, since finer particles ($PM_{2.5}$) are generated more due to human activities than relatively coarser particles (PM_{10}). During our study period, average PMr over all stations was varied between 0.40 (during July 2016) and 0.78 (during January 2013). PMr values were noted higher than 0.5 over 9 out of 11 sites; specifically, it was above 0.6 over the sites in Barisal (0.65), Dhaka (0.61) and Gazipur (0.60) which reveal that anthropogenic activities are more responsible for air pollution particularly at these sites. On the other hand, PMr value was lesser than 0.5 over Narayanganj (0.45) and Rajshahi (0.44) depicts higher meteorological

Table 1 Descriptive statistics of parameters used model experiments

Descriptive statistics	$PM_{2.5}$	PM_{10}	AT	RF	RH	AOD
Mean	89.13	152.17	25.19	2.41	70.74	0.96
Median	79.98	151.06	25.78	1.03	70.48	0.86
Mode	113.00	247.00	19.80	0.08	70.40	1.94
Standard deviation	56.26	84.68	3.70	3.03	9.32	0.62
Standard error	3.36	5.06	0.23	0.20	0.56	0.04
Range	244.30	366.70	15.80	12.66	47.26	2.10
Minimum	14.70	34.30	16.70	0.01	45.44	0.11
Maximum	259.00	401.00	32.50	12.67	92.70	2.21

influence on PM concentration. It is worth to mention these particular 2 sites are located within 1 km distance from large river bodies (Rajshahi on the bank of Padma river and Narayanganj on the bank of Shitalakshya river); therefore, continuous supply of water vapour with latent heat coming from river bodies might lead to secondary formation of PM and $PM_{2.5}$-PM_{10} conversion that results PMr value to be lesser than 0.5.

3.2 *MODIS$_{AOD}$ over CAMS sites*

More than 65% $MODIS_{AOD}$ were found comparable to $AERONET_{AOD}$ within EE followed in this study. Validation between $MODIS_{AOD}$ and $AERONET_{AOD}$ shows good matching over Dhaka ($R^2 = 0.72$, RMSE = 0.23). Spatial distribution of annually mean $MODIS_{AOD}$ during 2013–2018 (Fig. 1) shows comparatively high values over Rajshahi subdivision (0.69 ± 0.06) followed by Khulna (0.66 ± 0.09) and Dhaka (0.65 ± 0.08), while least over Chittagong (0.45 ± 0.14) followed by Sylhet (0.55 ± 0.08), therefore depicting higher pollution level in central and west Bangladesh. Seasonal mean of $MODIS_{AOD}$ ranges 0.29–0.83. The CAMS sites located in Dhaka and Chittagong register the seasonal pattern of AOD as $AOD_{summer} > AOD_{autumn} > AOD_{winter}$, whereas the sites in Gazipur and Narayanganj experience $AOD_{summer} > AOD_{winter} > AOD_{autumn}$; however, the sites in Khulna and Rajshahi register $AOD_{winter} > AOD_{summer} > AOD_{autumn}$. Thus, it depicts the influence of varying meteorological conditions on the spatial variability of AOD in different seasons. It also indicates that around industrial area the pollution level increases when the temperature is lower (winter), while traffic-induced pollution levels accelerate in megacities during comparatively hotter days (summer). During the rainy season, since high-quality AOD data pixels are very less due to cloud contaminations, most of the AOD values were missing.

3.3 Intra-annual pattern of PM, AOD and meteorology

Within 6 years of observation, no significant trend or interannual pattern can be perceived. However, analysis of intra-annual (monthly) pattern for these parameters shows better perspective. Monthly pattern of PM (Fig. 3a) reveals that January is the most polluted month ($PM_{2.5} = 167.75 \pm 35.81$ µg m^{-3}, $PM_{10} = 257.83 \pm 53.37$ µg m^{-3}) and August is the least polluted month ($PM_{2.5} = 23.77 \pm 5.26$ µg m^{-3}, $PM_{10} = 47.5 \pm 11.08$ µg m^{-3}). Earlier, [104] showed with the help of clustered trajectories that winter season in Bangladesh usually experienced significantly elevated concentration of secondary particulate matter due to the incursion of transboundary pollution through the inflow of continental air masses mostly from the Ganga–Brahmaputra plain in India. Concurrently, the monthly mean value of PMr was found highest during January (0.65) and lowest during July (0.47) with an annual average of 0.53. It indicates a higher anthropogenic contribution to the air pollution during winter days in this country and hence agreed to [105]. Monthly pattern of $MODIS_{AOD}$ and RH (Fig. 3b) shows highest values of AOD during May (0.98) and lowest during August (0.36), whereas RH was highest during July (82.68%) and lowest during March (62.59%). It is worth to mention that AOD found to be decreased with rise in RH during June–September but increased during March–May in spite of increase in RH. In addition, December was identified as the driest and coldest month (mean RF = 0.30 cm, mean AT = 20.59 °C), while June as the warmest month (mean AT = 28.76 °C) and July as the most humid month (mean RF = 9.05 cm, mean RH = 82.68%) (Fig. 3c). Thus, the monthly pattern suggests that during January–April, the difference between $PM_{2.5}$ and PM_{10} concentration was > 90 µg m^{-3}, i.e. 1.5 times higher than any other month in a year, during those particular months, AT was rising at rate of > 1.5 °C/month, but average RH remains lesser than 65% and 1.2 cm, respectively, therefore suggesting that the prevailing meteorological conditions during this particular transitional period (from winter to summer) are highly affecting the physio-chemical transformation of $PM_{2.5}$ to PM_{10} as there is least chance of dust influence in Bangladesh; rather than that, the large network of rivers and other inland water bodies might have provided immense supply of heat and moisture during these months which might trigger secondary formation of PM_{10}; hence, such high rise in PM_{10} was observed in these months.

3.4 Model experiments for PM estimation

The performance of experimented 8 regression models, in terms of R^2, NRMSE, NMB, is shown in Table 2. The simple linear regression (*M*1) shows considerably lower value of R^2 (< 0.05) and higher NRMSE (> 0.5) for both of $PM_{2.5}$ and PM_{10}, therefore signifying that the ground-level PM cannot be estimated only by using AOD (Fig. 4a). Multiple linear regression model (*M*2) accounts meteorological parameters along with AOD and showed R^2 value of 0.64 for $PM_{2.5}$ and 0.67 for PM_{10} (Fig. 4b) which suggest an unavoidable importance of meteorological parameters while estimating the PM. However, it exhibits higher estimation error—NRMSE of 0.42 for $PM_{2.5}$ and 0.32 for PM_{10}. Thereafter, SVR models were experimented where both of 'nu' and 'eps' type of regression techniques were tested for each 3 kernels. Using linear kernel, *M*3 (Fig. 4c) and *M*6 (Fig. 4d) showed moderate estimation accuracy ($0.5 \le R^2 \le 0.6$); hence, it indicates the nonlinearity in the

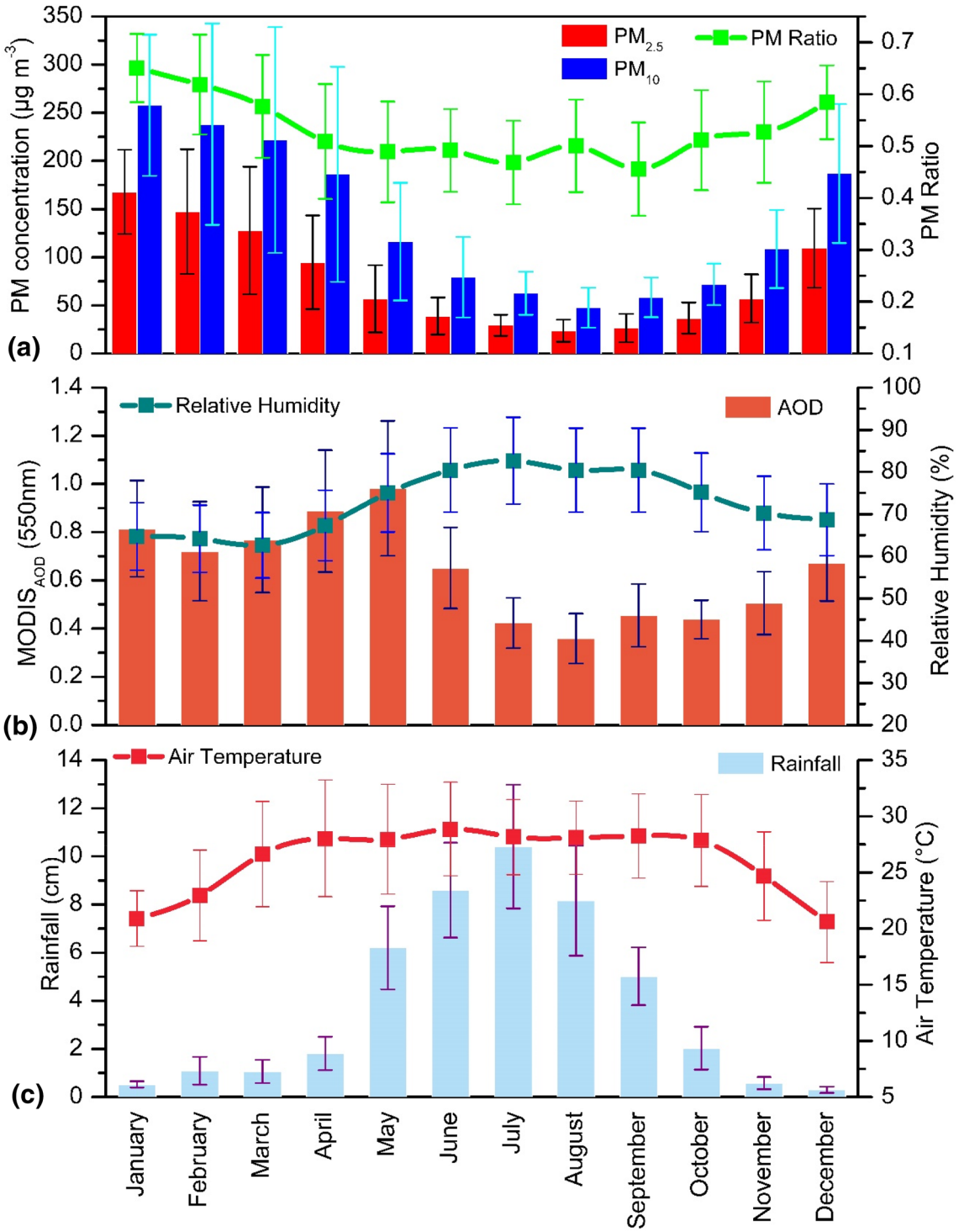

Fig. 3 Intra-annual pattern of (**a**) ground measured PM concentration, (**b**) MODIS - AOD, (**c**) meteorology over CAMS locations. Error bars represent ± 1σ for each monthly mean observation

dataset, while applying the polynomial kernel of 3rd degree in *M*4 (Fig. 4e) and *M*7 (Fig. 4f), the estimation accuracy reduced drastically ($0.15 \le R^2 \le 0.30$). The poorer performance of polynomial kernel probably suggests that the observations in training dataset are not standardized; in other words, higher degrees of fluctuations exist in the dataset. The radial kernel-based 'eps' regression model (*M*5) is found to be the outperformer (Fig. 4g) among all

Table 2 Evaluation of experimented models

Model No	Model type	$PM_{2.5}$ estimation			PM_{10} estimation		
		R^2	NMB	NRMSE	R^2	NMB	NRMSE
M1	Univariate	0.01	0.03	0.61	0.04	0.01	0.53
M2	Multivariate	0.64	0.05	0.42	0.67	0.05	0.32
M3	SVR-eps-linear kernel	0.50	−0.02	0.41	0.58	0.03	0.42
M4	SVR-eps-polynomial kernel	0.15	0.06	0.45	0.28	0.07	0.48
M5	SVR-eps-radial kernel	0.84	0.01	0.20	0.85	0.02	0.23
M6	SVR-nu-linear kernel	0.49	0.01	0.45	0.60	0.02	0.40
M7	SVR-nu-polynomial kernel	0.18	−0.02	0.46	0.24	−0.01	0.47
M8	SVR-nu-radial kernel	0.77	0.01	0.21	0.79	0.02	0.28

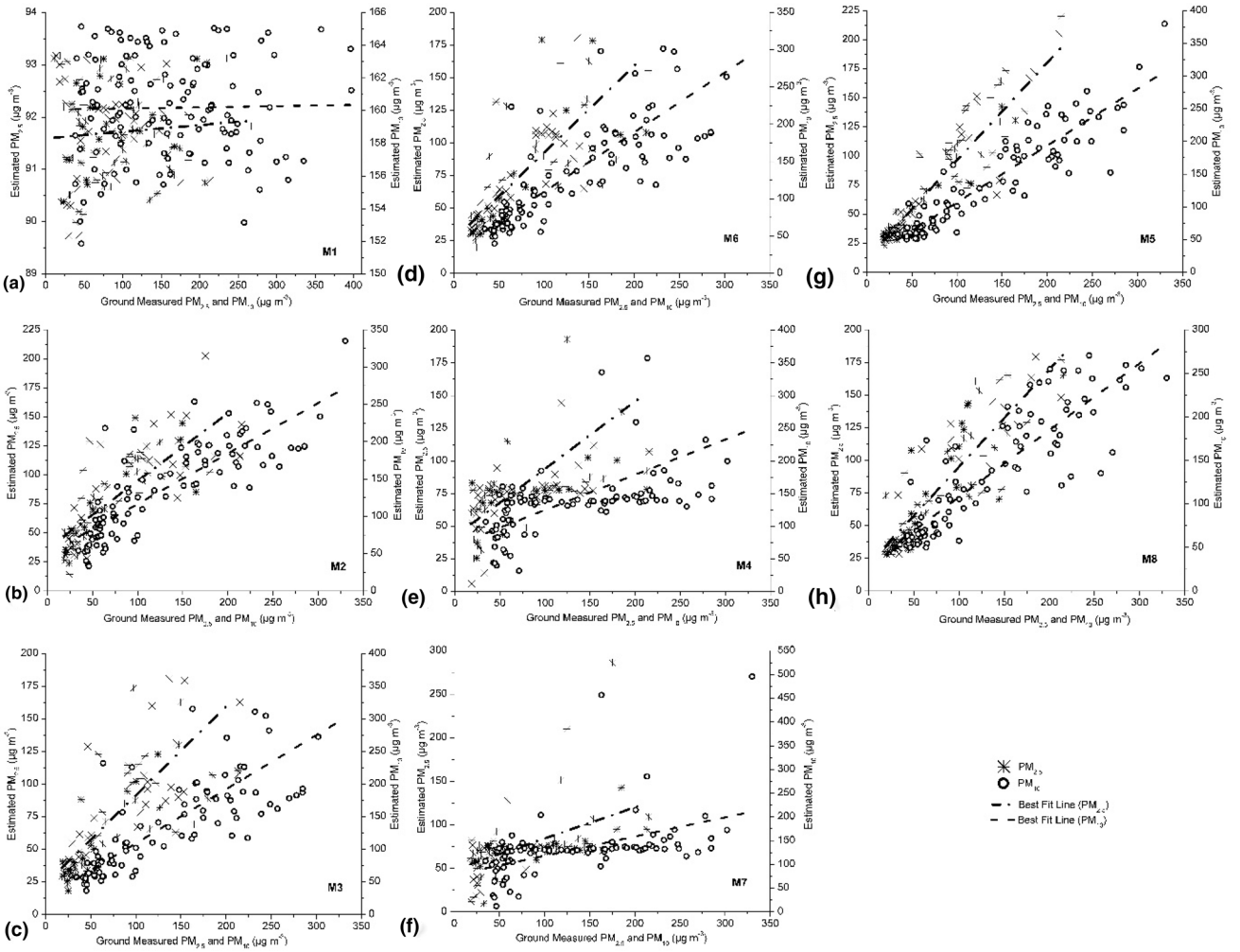

Fig. 4 Validation of experimented models

the experimented models, slightly better than 'nu'-based regression model (*M8*) (Fig. 4h). In *M5*, R^2 value achieved for $PM_{2.5}$ and PM_{10} was 0.84 and 0.85 successively, whereas for *M8* it was 0.77 and 0.79 sequentially. The NRMSE and NMB were also lesser than 0.25 and ± 0.05, respectively, in *M5*. Noteworthy, PM_{10} was able to estimate with a little better accuracy than $PM_{2.5}$. Therefore, it conjectured that using SVR models, estimation accuracy does not vary much over the type of regression, rather the selection of kernel matters. It also surmises that due to stationary property, radial kernel yields the input values in much higher dimensions than other kernels do as well as it trains the

model taking Euclidean distance from each respective data point, thus improving the estimation accuracy in such complex coherence of AOD, PM and meteorology.

3.5 Interrelation of meteorological parameters with PM and AOD

Model experiments have firmly declared that higher PM estimation accuracy can be achieved only when the meteorological parameters are included as input; however, it is also important to check how much each meteorological parameters are influencing the model accuracy. Thus, the best performed model, i.e. *M*5, was re-experimented with several iterations keeping each one alternative input parameter off (Table 3). Considering only AOD as input, R^2 value found to be very poor in *M*5a (0.11 for $PM_{2.5}$ and 0.10 for PM_{10}). By including only AT with AOD as input (*M*5b), the R^2 value increased up to 0.60 and 0.54 for $PM_{2.5}$ and PM_{10} estimation, respectively, while taking only RH with AOD as input (*M*5c), R^2 value increased up to 0.46 and 0.52 for $PM_{2.5}$ and PM_{10} estimation successively. However, comparatively lesser improvement in R^2 value (0.25 for $PM_{2.5}$ and 0.26 for PM_{10} estimation) was noticed when RF and AOD were considered as input (*M*5d). Moreover, with an input combination of AOD-AT-RH (*M*5e), 0.80 of R^2 value was achieved for both of $PM_{2.5}$ and PM_{10} estimation, which was better than AOD-AT-RF (*M*5f) and AOD-RH-RF (*M*5g) combinations. The accuracy increased further, while all 3 meteorological parameters with AOD had been taken as input (*M*5), thus depicting that AT has major importance followed by RH and RF. Interestingly, all meteorological parameters were found to be negatively correlated with ground measurement of $PM_{2.5}$ (Fig. 5a–c) and PM_{10} (Fig. 5d–f) over CAMS locations, likewise observed by [106]. Correlation with AT for both of $PM_{2.5}$ ($r=-0.80$) and PM_{10} ($r=-0.73$) concentration was found to be better than RH ($r=-0.66$, $r=-0.73$) and RF ($r=-0.59$, $r=-0.61$), respectively. Analysis also reveals that PM_{10} is better associated with RH and RF than $PM_{2.5}$, while AT is more sensitive to $PM_{2.5}$ than PM_{10}. Hence, it limned that during cooler and drier days, the PM concentration tends to increase, while higher precipitation and humidity result in significant improvement (decrease) in PM pollution. On the other hand, over the monitoring stations, $MODIS_{AOD}$ registered positive correlation with AT ($r=0.66$) (Fig. 5g), but negative correlation with RH ($r=-0.59$) (Fig. 5h) and RF ($r=-0.72$) (Fig. 5i), thus signifying that $MODIS_{AOD}$ exhibits tendency to show higher values on drier and hotter days but lesser values in humid conditions. During the warmer days, due to the gas-particle transformation occurred high above the surface results in higher concentration of aerosol which could be depicted by columnar measurement of AOD [107], while at the same time, due to higher surface air temperature, the convection process near the ground amplifies, and thus the convective air lugged the surface PM concentration away [108] which results into comparatively lesser value of surface PM.

4 Conclusion

The overall study based on ground observations of PM exhibits that the annual mean $PM_{2.5}$ and PM_{10} concentration is approximately 1.2–1.75 times higher than the BNAAQS (50 μg m^{-3} for $PM_{2.5}$ and 100 μg m^{-3} for PM_{10}) over all the monitoring locations; therefore, the people residing in those urban areas around CAMS sites are inhaling extremely bad air, especially during the nonrainy seasons when PM concentrations are recorded approximately 2–5 times higher than the given BNAAQs safety limit. The adverse effect of such terrible air quality has already been noticed over Dhaka, since the cardiac diseases are

Table 3 Experiments with several combinations of meteorological input to estimate PM and their evaluation

Model no	*M*5a	*M*5b	*M*5c	*M*5d	*M*5e	*M*5f	*M*5g	*M*5
Parameters	AOD	AOD	AOD	AOD	AOD	AOD	AOD	AOD
		AT	RH	RF	AT	AT	RH	AT
					RH	RF	RF	RH
								RF
$PM_{2.5}$								
R^2	0.11	0.60	0.46	0.25	0.80	0.62	0.49	0.84
NMB	0.07	0.04	0.01	0.05	0.02	0.04	0.01	0.01
NRMSE	0.29	0.22	0.25	0.16	0.28	0.22	0.24	0.23
PM_{10}								
R^2	0.10	0.54	0.52	0.26	0.80	0.60	0.57	0.85
NMB	0.06	0.02	0.01	0.04	0.01	0.02	0.03	0.02
NRMSE	0.34	0.19	0.29	0.22	0.27	0.29	0.25	0.23

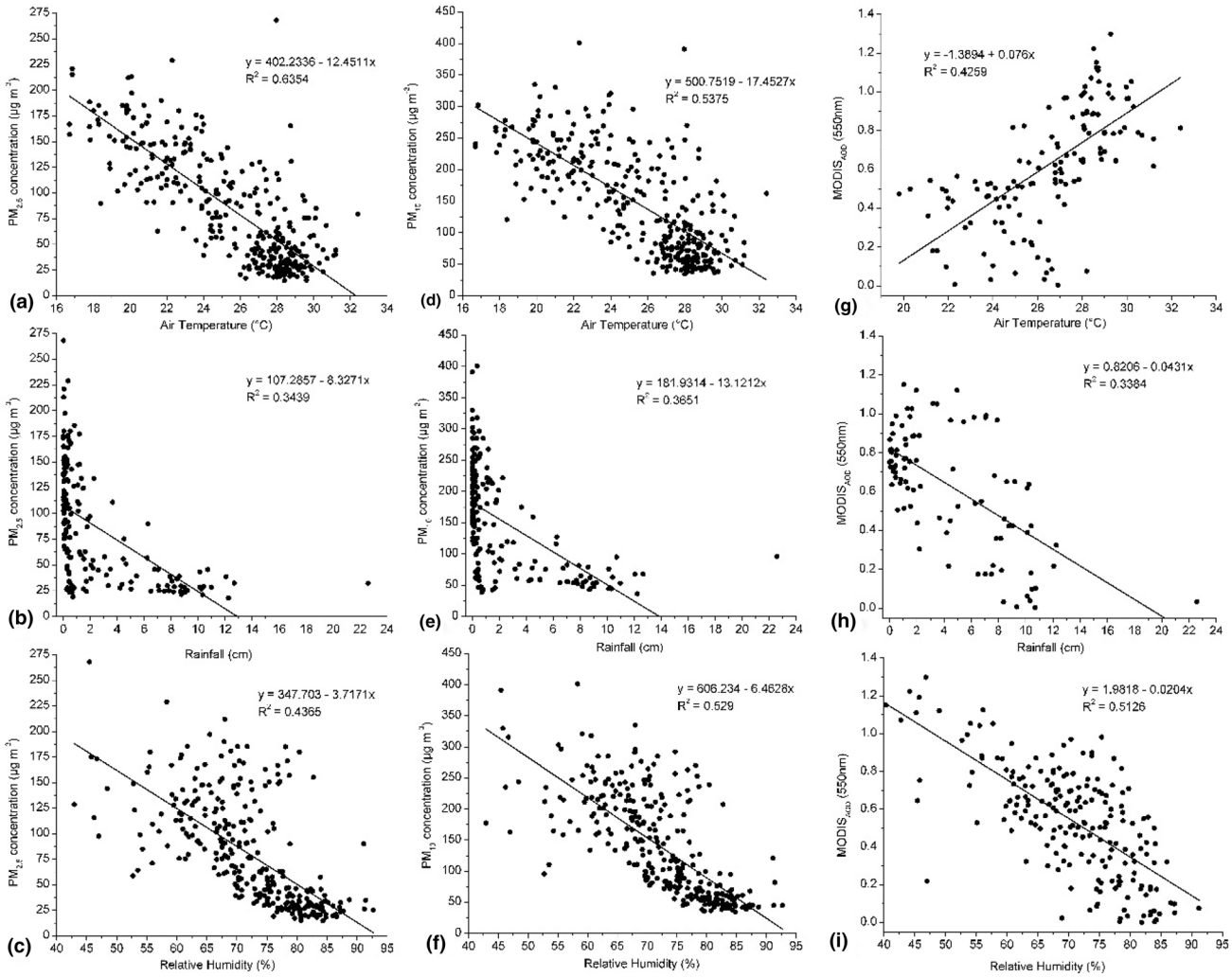

Fig. 5 Interrelation between meteorological parameters and (**a–c**) $PM_{2.5}$, (**d–f**) PM_{10}, (**g–i**) MODIS-AOD

noted to be increased in the city [109]. The shortening of life expectancy caused by the hazardous air quality has been reported throughout the world [110–114]. In Bangladesh, more than 80 million population are young aged [82]; hence, there is very high chance that majority of the peoples in Bangladesh got affected by different diseases caused directly or indirectly by air pollution. However, all of the CAMS sites are located in urban areas only; therefore, the PM variations over rural sites could not be explored in the present study. In the study by [115], we have noticed the rapid urban expansion of major cities in Bangladesh, which also make a crucial impact in severity of air pollution. Thus, the current scenario urges high attention of policy makers to take preventive measures precociously in order to get control over such worse pollution scenario, especially during winter.

The present study has drawn a crystal clear conclusion about nonsignificant correlation between satellite-measured AOD and ground-observed PM as well as illustrates the essentiality to take meteorology in to consideration in order to improve the accuracy of PM estimation in the context of Bangladesh. Greater coverage of ground network would have given more detailed information about PM-AOD interrelationship. Therefore, with proper network of meteorological observations and utilizing satellite data it will be very helpful to monitor air pollution level over any specific region. Intra-annual pattern reveals that high RF and RH cause the PM and AOD level to decrease by the aerosol scavenging process only when there is no such variation in AT [116, 117], but during the autumn and winter months when all of AT, RF and RH decrease continuously, the pollution level got increased due to lesser deposition. During summer months when there was rapid increase in both of AT and RH, but comparatively less increase in RF, the physio-chemical transformations in PM also got increased which results increase in PM

level with remarkably high increase of AOD. However, statistically significant negative correlation for both of $PM_{2.5}$ and PM_{10} with each meteorological parameters agreed previous studies carried by [118–120]. Moreover, the study has found AT to be better correlated with $PM_{2.5}$ than PM_{10}, while RH and RF correlated better with PM_{10} than $PM_{2.5}$. Analysis propounds that the radial kernel-based SVR can be able to surmount the complexity of PM estimation and sequel the importance of meteorology as AT > RH > RF. Thus, it recommends usefulness of machine learning technique in air quality studies over the spatial context of Bangladesh. It can be used as operational method for daily or even real-time estimation of PM, depending on the retrieval process of AOD and frequency of meteorological observations with proper network of ground coverage

Acknowledgement Authors are acknowledged to Ministry of Environment and Forests, Bangladesh, for providing necessary ground data as well as LP DAAC from where satellite data have been obtained. Dr. Partha Mahapatra and Mr. Sumit Das are also acknowledged for their valuable advices to improve the article.

Compliance with ethical standards

Conflicts of interest The authors declare that they have no conflict of interest.

References

1. Peters A, Dockery DW, Muller JE, Mittleman MA (2001) Increased particulate air pollution and the triggering of myocardial infarction. Circ 103:2810–2815. https://doi.org/10.1161/01.CIR.103.23.2810
2. Rahman MM, Saidi K, Mbarek MB (2020) Economic growth in South Asia the role of CO_2 emissions, population density and trade openness. Heliyon 6(5):e03903
3. Chen M-J, Yang P-H, Hsieh M-T et al (2018) Machine learning to relate $PM_{2.5}$ and PM_{10} concentrations to outpatient visits for upper respiratory tract infections in Taiwan: a nationwide analysis. World J Clin C 6(8):200–206
4. He Y, Gao Z, Guo T et al (2018) Fine particulate matter associated mortality burden of lung cancer in Hebei Province, China: ten years of $PM_{2.5}$ and LC mortality. Thorac Cancer 9:820–826. https://doi.org/10.1111/1759-7714.12653
5. Hoek G, Raaschou-Nielsen O (2014) Impact of fine particles in ambient air on lung cancer. Chin J Cancer. https://doi.org/10.5732/cjc.014.10039
6. Lim J-M, Jeong J-H, Lee J-H et al (2011) The analysis of $PM_{2.5}$ and associated elements and their indoor/outdoor pollution status in an urban area: indoor/outdoor pollution of $PM_{2.5}$ and elements. Indoor Air 21:145–155. https://doi.org/10.1111/j.1600-0668.2010.00691.x
7. Manisalidis I, Stavropoulou E, Stavropoulos A, Bezirtzoglou E (2020) Environmental and health impacts of air pollution: a review. Front Public Health 8:14. https://doi.org/10.3389/fpubh.2020.00014
8. Hong C, Zhang Q, Zhang Y, Davis SJ, Tong D, Zheng Y, Liu Z, Guan D, He K, Schellnhuber HJ (2019) Impacts of climate change on future air quality and human health in China. Proc Nat Acad Sci 116(35):17193–17200. https://doi.org/10.1073/pnas.1812881116
9. Saliba NA, El Jam F, El Tayar G, Obeid W, Roumie M (2010) Origin and variability of particulate matter (PM_{10} and $PM_{2.5}$) mass concentrations over an Eastern Mediterranean city. Atmos Res 97:106–114. https://doi.org/10.1016/j.atmosres.2010.03.011
10. Sloss LL, Smith IM (2000) PM_{10} and $PM_{2.5}$: an international perspective. Fuel Process Technol 65–66:127–141. https://doi.org/10.1016/S0378-3820(99)00081-8
11. Vautard R, Builtjes PHJ, Thunis P, Cuvelier C, Bedogni M, Bessagnet B et al (2007) Evaluation and intercomparison of Ozone and PM_{10} simulations by several chemistry transport models over four European cities within the City Delta project. Atmos Environ 41:173–188. https://doi.org/10.1016/j.atmosenv.2006.07.039
12. Dumka UC, Kasakaoutis DG, Srivastava MK, Devara PCS (2015) Scattering and absorption properties of near-surface aerosol over Gangetic-Himalayan region: the role of boundary-layer dynamics and long-range transport. Atmos Chem Phys 15:1555–1572
13. Nanda C, Kant Y, Gupta A, Mitra D (2018) Spatio temporal distribution of pollutant trace gases during diwali over India. ISPRS Ann Photogramm Remote Sens Spatial Inf Sci IV–5:339–350
14. Prabhu V, Soni A, Madhwal S, Gupta A, Sundriyal S, Shridhar V, Sreekanth V et al (2020) Black carbon and biomass burning associated high pollution episodes observed at Doon valley in the foothills of the Himalayas. Atmos Res 243:105001. https://doi.org/10.1016/j.atmosres.2020.105001
15. Weaver AM, Gurley ES, Crabtree-Ide C, Salje H, Yoo E-H, Mu L et al (2019) Air pollution dispersion from biomass stoves to neighboring homes in Mirpur, Dhaka Bangladesh. BMC Public Health 19:425. https://doi.org/10.1186/s12889-019-6751-z
16. Bari MdA, Kindzierski WB (2018) Characterization of air quality and sources of fine particulate matter ($PM_{2.5}$) in the City of Calgary. Can Atmos Pollut Res 9:534–543. https://doi.org/10.1016/j.apr.2017.11.014
17. Elf JL, Kinikar A, Khadse S et al (2018) Sources of household air pollution and their association with fine particulate matter in low-income urban homes in India. J Expo Sci Environ Epidemiol 28:400–410. https://doi.org/10.1038/s41370-018-0024-2
18. Kundu S, Stone EA (2014) Composition and sources of fine particulate matter across urban and rural sites in the Midwestern United States. Environ Sci: Process Impacts 16:1360–1370. https://doi.org/10.1039/C3EM00719G
19. Seneviratne S, Handagiripathira L, Sanjeevani S, Madusha D, Waduge VAA, Attanayake T et al (2017) Identification of sources of fine particulate matter in Kandy, Sri Lanka. Aerosol Air Qual Res 17:476–484. https://doi.org/10.4209/aaqr.2016.03.0123
20. Weagle CL, Snider G, Li C, van Donkelaar A, Philip S, Bissonnette P et al (2018) Global sources of fine particulate matter: interpretation of $PM_{2.5}$ chemical composition observed by SPARTAN using a global chemical transport model. Environ Sci. https://doi.org/10.1021/acs.est.8b01658
21. Cho H-S, Choi M (2014) Effects of compact urban development on air pollution: empirical evidence from Korea. Sustain 6:5968–5982. https://doi.org/10.3390/su6095968
22. Liu X (2019) Effects of urban density and city size on haze pollution in China: spatial regression analysis based on 253 prefecture-level Cities $PM_{2.5}$ data. Discrete Dyn Nat Soc 2019:1–8. https://doi.org/10.1155/2019/6754704
23. Moore M, Gould P, Keary BS (2003) Global urbanization and impact on health. Int J Hyg Environ Health 206:269–278. https://doi.org/10.1078/1438-4639-00223
24. Power AL, Tennant RK, Jones RT, Tang Y, Du J, Worsley AT et al (2018) Monitoring impacts of urbanisation and industrialisation on air quality in the anthropocene using urban pond

sediments. Front Earth Sci 6:131. https://doi.org/10.3389/feart.2018.00131
25. Zhou C, Li S, Wang S (2018) Examining the impacts of urban form on air pollution in developing countries: a case study of China's Megacities. Int J Environ Res Public Health 15:1565. https://doi.org/10.3390/ijerph15081565
26. Dong X, Zhao X, Peng F, Wang D (2020) Population based air pollution exposure and its influence factors by integrating air dispersion modeling with GIS spatial analysis. Sci Rep. https://doi.org/10.1038/s41598-019-57385-9
27. Hasnat GNT, Kabir MA, Hossain MA (2018) Major Environmental Issues and Problems of South Asia Particularly Bangladesh, In Hussain C (eds) Handbook of Environmental Materials Management, Springer Cham 1–40 https://doi.org/10.1007/978-3-319-58538-3_7-1
28. Wang SX, Zhao B, Cai SY, Klimont Z, Nielsen CP, Morikawa T et al (2014) Emission trends and mitigation options for air pollutants in East Asia. Atmos Chem Phys 14:6571–6603. https://doi.org/10.5194/acp-14-6571-2014
29. Begum BA, Hopke PK, Markwitz A (2013) Air pollution by fine particulate matter in Bangladesh. Atmos Pollut Res 4:75–86. https://doi.org/10.5094/APR.2013.008
30. Islam MdS (2016) Air pollution in Dhaka City: a burning issue. J Sci Found 12:20–21. https://doi.org/10.3329/jsf.v12i2.27732
31. Mahmood A, Hu Y, Nasreen S, Hopke PK (2019) Airborne particulate pollution measured in Bangladesh from 2014–2017. Aerosol Air Qual Res 19:272–281. https://doi.org/10.4209/aaqr.2018.08.0284
32. Rouf M, Nasiruddin M, Hossain A, Islam M (2011) Trend of particulate matter $PM_{2.5}$ and PM_{10} in Dhaka City. Bangladesh J Sci Ind Res 46:389–398. https://doi.org/10.3329/bjsir.v46i3.9049
33. Rana MdM, Sulaiman N, Sivertsen B et al (2016) Trends in atmospheric particulate matter in Dhaka, Bangladesh, and the vicinity. Environ Sci Pollut Res 23:17393–17403. https://doi.org/10.1007/s11356-016-6950-4
34. Rahman MM, Mahamud S, Thurston GD (2019) Recent spatial gradients and time trends in Dhaka, Bangladesh, air pollution and their human health implications. J Air Waste Manag Assoc 69:478–501. https://doi.org/10.1080/10962247.2018.1548388
35. Gupta A, Kant Y, Mitra D, Chauhan P (2020) Spatio-temporal distribution of INSAT-3D AOD derived particulate matter concentration over India. Atmos Pollut Res. https://doi.org/10.1016/j.apr.2020.08.031
36. Chu DA (2006) Analysis of the relationship between MODIS aerosol optical depth and $PM_{2.5}$ in the summertime US. In: Chu A, Szykman J, Kondragunta S (eds) San Diego. California, USA, p 629903
37. Chudnovsky AA, Kostinski A, Lyapustin A, Koutrakis P (2013) Spatial scales of pollution from variable resolution satellite imaging. Environ Pollut 172:131–138. https://doi.org/10.1016/j.envpol.2012.08.016
38. Engel-Cox JA, Hoff RM, Haymet ADJ (2004) Recommendations on the use of satellite remote-sensing Data for urban air quality. J Air Waste Manag Assoc 54:1360–1371. https://doi.org/10.1080/10473289.2004.10471005
39. Kumar N, Chu A, Foster A (2007) An empirical relationship between $PM_{2.5}$ and aerosol optical depth in Delhi Metropolitan. Atmos Environ 41:4492–4503. https://doi.org/10.1016/j.atmosenv.2007.01.046
40. Li R, Gong J, Chen L, Wang Z (2015) Estimating ground-level $PM_{2.5}$ using fine-resolution satellite data in the megacity of Beijing. China Aerosol Air Qual Res 15:1347–1356. https://doi.org/10.4209/aaqr.2015.01.0009
41. Schaap M, Apituley A, Timmermans RMA, Koelemeijer RBA, Leeuw G (2009) Exploring the relation between aerosol optical depth and $PM_{2.5}$ at Cabauw, the Netherlands. Atmos Chem Phys 8(5):17939
42. Wang J, Christopher SA (2003) Intercomparison between satellite derived aerosol optical thickness and $PM_{2.5}$ mass: Implications for air quality studies. Geophys Res Lett. https://doi.org/10.1029/2003GL018174
43. You W, Zang Z, Pan X, Zhang L, Chen D (2014) Estimating $PM_{2.5}$ in Xi'an, China using aerosol optical depth: a comparison between the MODIS and MISR retrieval models. Sci Total Environ 505:1156–1165. https://doi.org/10.1016/j.scitotenv.2014.11.024
44. Kahn RA, Gaitley BJ (2015) An analysis of global aerosol type as retrieved by MISR: MISR aerosol Type. J Geophys Res Atmos 120:4248–4281. https://doi.org/10.1002/2015JD023322
45. Kaufman YJ, Tanré D, Boucher O (2002) A satellite view of aerosols in the climate system. Nat 419:215–223. https://doi.org/10.1038/nature01091
46. Remer LA, Kaufman YJ, Tanré D, Mattoo S, Chu DA, Martins JV et al (2005) The MODIS aerosol algorithm, products, and validation. J Atmos Sci 62:947–973. https://doi.org/10.1175/JAS3385.1
47. Torres O, Tanskanen A, Veihelmann B, Ahn C, Braak R, Bhartia PK et al (2007) Aerosols and surface UV products from Ozone monitoring instrument observations: an overview. J Geophys Res. https://doi.org/10.1029/2007JD008809
48. Winker DM, Pelon J, JAC JR, Ackerman SA, Charlson RJ, Colarco PR et al (2010) A global 3D view of aerosols and clouds. Bull Amer Meteor Soc 91(9):1211–1230
49. Levy RC, Mattoo S, Munchak LA et al (2013) The collection 6 MODIS aerosol products over land and ocean. Atmos Meas Tech 6:2989–3034. https://doi.org/10.5194/amt-6-2989-2013
50. Tanré D, Kaufman YJ, Herman M, Mattoo S (1997) Remote sensing of aerosol properties over oceans using the MODIS/EOS spectral radiances. J Geophys Res 102:16971–16988. https://doi.org/10.1029/96JD03437
51. Hsu NC, Tsay S-C, King MD, Herman JR (2004) Aerosol properties over bright-reflecting source regions. IEEE Trans Geosci Remote Sens 42:557–569. https://doi.org/10.1109/TGRS.2004.824067
52. Hsu NC, Jeong M-J, Bettenhausen C et al (2013) Enhanced deep blue aerosol retrieval algorithm: the second generation: enhanced deep blue aerosol retrieval. J Geophys Res Atmos 118:9296–9315. https://doi.org/10.1002/jgrd.50712
53. Lyapustin A, Martonchik J, Wang Y et al (2011) Multiangle implementation of atmospheric correction (MAIAC): 1 radiative transfer basis and look up tables. J Geophys Res. https://doi.org/10.1029/2010JD014985
54. Lyapustin A, Wang Y, Laszlo I et al (2011) Multiangle implementation of atmospheric correction (MAIAC): 2. Aerosol algorithm J Geophys Res 116:D03211. https://doi.org/10.1029/2010JD014986
55. Lyapustin A, Wang Y, Laszlo I et al (2012) Multi-angle implementation of atmospheric correction for MODIS (MAIAC): 3. Atmos correct Remote Sens of Environ 127:385–393. https://doi.org/10.1016/j.rse.2012.09.002
56. Gupta P, Christopher SA (2009) Particulate matter air quality assessment using integrated surface, satellite, and meteorological products: 2 a neural network approach. J Geophys Res. https://doi.org/10.1029/2008JD011497
57. Gupta P, Christopher SA, Wang J et al (2006) Satellite remote sensing of particulate matter and air quality assessment over global cities. Atmos Environ 40:5880–5892. https://doi.org/10.1016/j.atmosenv.2006.03.016
58. He Q, Zhou G, Geng F et al (2016) Spatial distribution of aerosol hygroscopicity and its effect on $PM_{2.5}$ retrieval in East China. Atmos Res 170:161–167. https://doi.org/10.1016/j.atmosres.2015.11.011

59. Karimian H, Li Q, Li C et al (2016) An improved method for monitoring fine particulate matter mass concentrations via Satellite Remote Sensing. Aerosol Air Qual Res 16:1081–1092. https://doi.org/10.4209/aaqr.2015.06.0424
60. Lin C, Li Y, Yuan Z et al (2015) Using satellite remote sensing data to estimate the high-resolution distribution of ground-level $PM_{2.5}$. Remote Sens Environ 156:117–128. https://doi.org/10.1016/j.rse.2014.09.015
61. Sinha PR, Gupta P, Kaskaoutis DG, Sahu LK, Nagendra N, Manchanda RK, Kumar YB, Sreenivasan S (2015) Estimation of particulate matter from satellite- and ground-based observations over Hyderabad. India Int J Remote Sens 36(24):6192–6213. https://doi.org/10.1080/01431161.2015.1112929
62. Yang Q, Yuan Q, Li T, Shen H, Zhang L (2017) The relationships between $PM_{2.5}$ and meteorological factors in China: seasonal and regional variations. Int J Environ Res Public Health. https://doi.org/10.3390/ijerph14121510
63. Koelemeijer RBA, Homan CD, Matthijsen J (2006) Comparison of spatial and temporal variations of aerosol optical thickness and particulate matter over Europe. Atmos Environ 40:5304–5315. https://doi.org/10.1016/j.atmosenv.2006.04.044
64. Lin J, van Donkelaar A, Xin J et al (2014) Clear-sky aerosol optical depth over East China estimated from visibility measurements and chemical transport modeling. Atmos Environ 95:258–267. https://doi.org/10.1016/j.atmosenv.2014.06.044
65. Tian J, Chen D (2010) A semi-empirical model for predicting hourly ground-level fine particulate matter ($PM_{2.5}$) concentration in southern Ontario from satellite remote sensing and ground-based meteorological measurements. Remote Sens Environ 114:221–229. https://doi.org/10.1016/j.rse.2009.09.011
66. Liu Y, Franklin M, Kahn R, Koutrakis P (2007) Using aerosol optical thickness to predict ground-level $PM_{2.5}$ concentrations in the St. Louis area: a comparison between MISR and MODIS. Remote Sens Environ 107:33–44. https://doi.org/10.1016/j.rse.2006.05.022
67. Liu Y, Sarnat JA, Kilaru V et al (2005) Estimating ground-level $PM_{2.5}$ in the Eastern United States using satellite remote sensing. Environ Sci Technol 39:3269–3278. https://doi.org/10.1021/es049352m
68. Sotoudeheian S, Arhami M (2014) Estimating ground-level PM_{10} using satellite remote sensing and ground-based meteorological measurements over Tehran. J Environ Health Sci Eng 12(1):13. https://doi.org/10.1186/s40201-014-0122-6
69. Wallace J, Kanaroglou P (2007) An investigation of air pollution in southern Ontario, Canada, with MODIS and MISR Aerosol Data. 2007 IEEE International Geoscience and Remote Sensing Symposium. IEEE, Barcelona, Spain, pp 4311–4314
70. Zaman NAFK, Kanniah KD, Kaskaoutis DG (2017) Estimating particulate matter using satellite based aerosol optical depth and meteorological variables in Malaysia. Atmos Res. https://doi.org/10.1016/j.atmosres.2017.04.019
71. Liu Y, Paciorek CJ, Koutrakis P (2009) Estimating regional spatial and temporal variability of $PM_{2.5}$ concentrations using satellite data, meteorology, and land use information. Environ Health Perspect 117:886–892. https://doi.org/10.1289/ehp.0800123
72. Paciorek CJ, Liu Y (2009) Limitations of remotely sensed aerosol as a spatial proxy for fine particulate matter. Environ Health Perspect 117:904–909. https://doi.org/10.1289/ehp.0800360
73. Song Y-Z, Yang H-L, Peng J-H, Song Y-R, Sun Q, Li Y (2015) Estimating $PM_{2.5}$ concentrations in Xi'an City using a generalized additive model with multi-source monitoring data. PLoS ONE. https://doi.org/10.1371/journal.pone.0142149
74. Beloconi A, Kamarianakis Y, Chrysoulakis N (2016) Estimating urban PM_{10} and $PM_{2.5}$ concentrations, based on synergistic MERIS/AATSR aerosol observations land cover and morphology data. Remote Sens of Environ 172:148–164
75. Ma Z, Liu Y, Zhao Q et al (2016) Satellite-derived high resolution $PM_{2.5}$ concentrations in Yangtze River Delta Region of China using improved linear mixed effects model. Atmos Environ 133:156–164. https://doi.org/10.1016/j.atmosenv.2016.03.040
76. Zheng Y, Zhang Q, Liu Y, Geng G, He K (2016) Estimating ground-level $PM_{2.5}$ concentrations over three megalopolises in China using satellite-derived aerosol optical depth measurements. Atmos Environ 124:232–242. https://doi.org/10.1016/j.atmosenv.2015.06.046
77. Hu X, Waller LA, Al-Hamdan MZ et al (2013) Estimating ground-level $PM_{2.5}$ concentrations in the southeastern U.S. using geographically weighted regression. Environ Res 121:1–10. https://doi.org/10.1016/j.envres.2012.11.003
78. van Donkelaar A, Martin RV, Spurr RJD, Burnett RT (2015) High-resolution satellite-derived $PM_{2.5}$ from optimal estimation and geographically weighted regression over North America. Environ Sci Technol 49:10482–10491. https://doi.org/10.1021/acs.est.5b02076
79. Gupta A, Pradhan B (2020) Impact of daily weather on COVID-19 outbreak in India. Preprint in medRixv. https://doi.org/10.1101/2020.06.15.20131490
80. Weizhen H, Zhengqiang L, Yuhuan Z, Hua X, Ying Z, Kaitao L et al (2014) Using support vector regression to predict PM_{10} and $PM_{2.5}$. Earth Environ Sci, IOP Conf Ser. https://doi.org/10.1088/1755-1315/17/1/012268
81. Yeganeh B, Hewson MG, Clifford S, Knibbs LD, Morawska L (2017) A satellite-based model for estimating $PM_{2.5}$ concentration in a sparsely populated environment using soft computing techniques. Environ Model Softw 88:84–92. https://doi.org/10.1016/j.envsoft.2016.11.017
82. Farid K, Ahmed J, Sarma P, Begum S (2011) Population dynamics in Bangladesh: data sources, current facts and past trends. J Bangladesh Agric Univ 9:121–130. https://doi.org/10.3329/jbau.v9i1.8754
83. Rana MdM, Biswas SK (2019) Ambient air quality in Bangladesh 2012–2018. https://doi.org/https://doi.org/10.13140/RG.2.2.14741.17128
84. Mahapatra PS, Sinha PR, Boopathy R et al (2018) Seasonal progression of atmospheric particulate matter over an urban coastal region in peninsular India: role of local meteorology and long-range transport. Atmos Res 199:145–158. https://doi.org/10.1016/j.atmosres.2017.09.001
85. Tiwari S, Dumka UC, Gautam AS, Kaskaoutis DG, Srivastava AK, Bisht DS (2016) Assessment of $PM_{2.5}$ and PM_{10} over Guwahati in Brahmaputra river valley temporal evolution source apportionment and meteorological dependence. Atmos Pollut Res. https://doi.org/10.1016/j.apr.2016.07.008
86. Sinha PR, Manchanda RK, Kaskaoutis DG, Sreenivasan S, Moorthy KK, Babu SS (2011) Spatial heterogeneities in aerosol size distribution over Bay of Bengal during Winter-ICARB Experiment. Atmos Environ 45:4695–4706. https://doi.org/10.1016/j.atmosenv.2011.04.085
87. Khan MHR, Rahman A, Luo C et al (2019) Detection of changes and trends in climatic variables in Bangladesh during 1988–2017. Heliyon 5:e01268. https://doi.org/10.1016/j.heliyon.2019.e01268
88. Rashid HE (2019) Geography of Bangladesh. Routledge. https://doi.org/10.4324/9780429048098
89. Lyapustin A, Wang Y, Korkin S, Huang D (2018) MODIS collection 6 MAIAC algorithm. Atmos Meas Tech 11:5741–5765. https://doi.org/10.5194/amt-11-5741-2018
90. Lyapustin A, Alexander MJ, Ott L et al (2014) Observation of mountain lee waves with MODIS NIR column water vapor: lyapustin et al.: mountain waves in MODIS NIR water vapor. Geophys Res Lett 41:710–716. https://doi.org/10.1002/2013GL058770

91. Holben BN, Eck TF, Slutsker I et al (1998) AERONET—A federated instrument network and data archive for aerosol characterization. Remote Sens Environ 66:1–16. https://doi.org/10.1016/S0034-4257(98)00031-5
92. Chu Y, Liu Y, Li X et al (2016) A review on predicting ground $PM_{2.5}$ concentration using satellite aerosol optical depth. Atmos 7:129. https://doi.org/10.3390/atmos7100129
93. Chudnovsky AA, Koutrakis P, Kloog I et al (2014) Fine particulate matter predictions using high resolution aerosol optical depth (AOD) retrievals. Atmos Environ 89:189–198. https://doi.org/10.1016/j.atmosenv.2014.02.019
94. Soni M, Payra S, Verma S (2018) Particulate matter estimation over a semi arid region Jaipur, India using satellite AOD and meteorological parameters. Atmos Pollut Res 9:949–958. https://doi.org/10.1016/j.apr.2018.03.001
95. Vapnik V, Golowich SE, Smola AJ (1997) Support vector method for function approximation, Regres estim Signal Process. 7
96. Vapnik VN (1995) The nature of statistical learning Theory. Springer, New York
97. Cortes C, Vapnik V (1995) Support-vector networks. Mach Learn 20:273–297. https://doi.org/10.1007/BF00994018
98. Smola AJ, Schölkopf B (2004) A tutorial on support vector regression. Stat Comput 14:199–222. https://doi.org/10.1023/B:STCO.0000035301.49549.88
99. Liu L, Shen B, Wang X (2014) Research on kernel function of support vector machine. In: Huang Y-M, Chao H-C, Deng D-J, Park JJ (eds) Advanced technologies, embedded and multimedia for human-centric computing. Springer, Netherlands, Dordrecht, pp 827–834
100. Ben-Hur A, Ong CS, Sonnenburg S et al (2008) Support Vector machines and kernels for computational biology. PLoS Comput Biol. https://doi.org/10.1371/journal.pcbi.1000173
101. Gupta A, Pradhan B, Maulud KNA (2020) Estimating the impact of daily weather on the temporal pattern of COVID-19 outbreak in India. Earth Sys Environ. https://doi.org/10.1007/s41748-020-00179-1
102. Huang H-Y, Lin C-J (2016) Linear and kernel classification: when to use which? In: Proc of the 2016 SIAM Int Conf Data Mining. Society for Industrial and Applied Mathematics, pp 216–224
103. Yekkehkhany B, Safari A, Homayouni S, Hasanlou M (2014) A comparison study of different kernel functions for Svm-based classification of multi-temporal polarimetry sar data. Int Arch Photogramm Remote Sens Spatial Inf Sci. https://doi.org/10.5194/isprsarchives-XL-2-W3-281-2014
104. Rana MM, Mahmud M, Khan MH, Sivertsen B, Sulaiman N (2016) Investigating incursion of transboundary pollution into the atmosphere of Dhaka. Advances in Meteorology, Bangladesh. https://doi.org/10.1155/2016/8318453
105. Azkar MAMBI, Chatani S, Sudo K (2012) Simulation of urban and regional air pollution in Bangladesh. J Geophy Res Atmos. https://doi.org/10.1029/2011JD016509
106. Dominick D, Latif MT, Juahir H et al (2012) An assessment of influence of meteorological factors on PM_{10} and NO_2 at selected stations in Malaysia. Sustain Environ Res 22:305–315
107. Filonchyk M, Yan H (2018) Urban air pollution monitoring by ground-based stations and satellite data: multi-season characteristics from Lanzhou City. Springer, China
108. Adam ME-N (2013) Suspended particulates concentration (PM_{10}) under unstable atmospheric conditions over subtropical urban area (Qena, Egypt). Adv in Meteorol 2013:e457181. https://doi.org/10.1155/2013/457181
109. Khan R, Konishi S, Ng CFS et al (2019) Association between short-term exposure to fine particulate matter and daily emergency room visits at a cardiovascular hospital in Dhaka, Bangladesh. Sci Total Environ 646:1030–1036. https://doi.org/10.1016/j.scitotenv.2018.07.288
110. Balakrishnan K, Dey S, Gupta T, Dhaliwal RS, Brauer M, Cohen AJ et al (2019) The impact of air pollution on deaths, disease burden, and life expectancy across the states of India: the Global Burden of Disease Study 2017. The Lancet Planet Health 3:e26–e39. https://doi.org/10.1016/S2542-5196(18)30261-4
111. Brunekreef B (1997) Air pollution and life expectancy: is there a relation? Occup Environ Med 54:781–784. https://doi.org/10.1136/oem.54.11.781
112. Hill TD, Jorgenson AK, Ore P et al (2019) Air quality and life expectancy in the United States: an analysis of the moderating effect of income inequality. SSM - Population Health 7:100346. https://doi.org/10.1016/j.ssmph.2018.100346
113. Wen M, Gu D (2012) Air pollution shortens life expectancy and health expectancy for older adults: the case of China. J Gerontol Series A: Biol Sci Medical Sci 67:1219–1229. https://doi.org/10.1093/gerona/gls094
114. Afsar B, Afsar ER, Kanbay A, Covic A, Ortiz A, Kanbay M (2019) Air pollution and kidney disease: review of current evidence. Clin Kidney J 12:19–32. https://doi.org/10.1093/ckj/sfy111
115. Moniruzzaman MD, Roy A, Bhatt CM, Gupta A, An NTT, Hassan MR (2018) Impact analysis of urbanization on land use land cover change for Khulna City, Bangladesh using temporal landsat imagery. Int Arch Photogramm Remote Sens Spatial Inf Sci. https://doi.org/10.5194/isprs-archives-XLII-5-757-2018
116. Chate DM, Rao PSP, Naik MS et al (2003) Scavenging of aerosols and their chemical species by rain. Atmos Environ 37:2477–2484. https://doi.org/10.1016/S1352-2310(03)00162-6
117. Luan T, Guo X, Zhang T, Guo L (2019) Below-cloud aerosol scavenging by different-intensity rains in Beijing City. J Meteorol Res 33:126–137. https://doi.org/10.1007/s13351-019-8079-0
118. Bhaskar BV, Mehta VM (2010) Atmospheric particulate pollutants and their relationship with meteorology in Ahmedabad. Aerosol Air Qual Res 10:301–315. https://doi.org/10.4209/aaqr.2009.10.0069
119. Hernandez G, Berry T-A, Wallis SL, Poyner D (2017) Temperature and humidity effects on particulate matter concentrations in a sub-tropical climate during winter. IPCBEE. https://doi.org/10.7763/IPCBEE.2017
120. Tai APK, Mickley LJ, Jacob DJ (2010) Correlations between fine particulate matter ($PM_{2.5}$) and meteorological variables in the United States: implications for the sensitivity of $PM_{2.5}$ to climate change. Atmos Environ 44:3976–3984. https://doi.org/10.1016/j.atmosenv.2010.06.060